JOURNAL OF CHEMICAL INFORMATION AND MODELING

Article

pubs.acs.org/jcim

Effect of Cholesterol on the Structure of Membrane-Attached Cytochrome P450 3A4

Veronika Navrátilová, Markéta Paloncýová, Michaela Kajšová, Karel Berka,* and Michal Otyepka*

Regional Centre of Advanced Technologies and Materials, Department of Physical Chemistry, Faculty of Science, Palacký University Olomouc, tř. 17. listopadu 12, 771 46, Olomouc, Czech Republic

Supporting Information

ABSTRACT: Cholesterol is a widely researched component of biological membranes that significantly influences membrane properties. Human cytochrome P450 3A4 (CYP3A4) is an important drug-metabolizing enzyme, wherein the catalytic domain is attached to a membrane by an N-terminal α-helical transmembrane anchor. We analyzed the behavior of CYP3A4 immersed in a 1,2-dioleoyl-*sn*-glycero-3-phosphocholine (DOPC) membrane with various amounts of cholesterol. The presence of cholesterol caused ordering and thickening of the membrane and led to greater immersion and inclination of CYP3A4 toward the membrane. Cholesterol also lowered the flexibility of and tended to concentrate around membrane-immersed parts of CYP3A4. Further, the pattern of the CYP3A4 active-site access channels was altered in the presence of cholesterol. In summary, cholesterol in the membrane affected the positioning and structural features of CYP3A4, which in turn may have implications for the activity of this enzyme in various membranes and membrane parts with different cholesterol content.

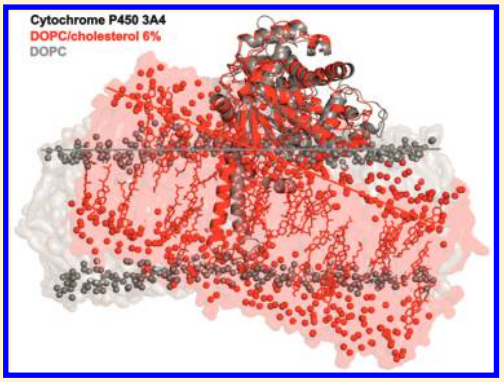

INTRODUCTION

Human cytochrome P450 (CYP) enzymes are involved in biotransformation processes of endogenous compounds and xenobiotics. Although they typically catalyze monooxygenation reactions, their catalytic potential is more diverse.[1,2] CYPs attach to membranes of the endoplasmic reticulum (ER) and mitochondria[3] by an N-terminal anchor, and their catalytic domains are partially immersed in the membrane.[4−6] It has been suggested that the membrane is not merely a passive medium but may actively contribute to the biotransformation processes by accumulation of nonpolar compounds.[7−9] Such compounds may also enter the CYP active site from the membrane via the active-site access channels.[5,6,9,10] The behavior of CYP on a membrane may be affected by the membrane composition and in turn the breathing (dynamical opening/closing) of access channels.[6,11] Moreover, CYP activity is dependent on the presence of certain redox partners, which attach to the membrane via transmembrane helices.[12,13] Thus, it is important to gain a deeper understanding of the role of membranes in the above-mentioned processes.

Direct structural insight into the behavior of membrane-anchored enzymes is still very challenging for experimental techniques. Until now, only NMR[14,15] and linear dichroism[16] measurements have been able to provide direct information on the membrane attachment of CYPs. It took more than 10 years after publication of the first X-ray structure of mammalian CYP[17] for the first crystal structure of CYP to be reported, which showed a resolved N-terminal anchor but only applied to outside the membrane environment.[18] However, it has been shown that missing information on the structural behavior of CYP on membrane can be gleaned by molecular dynamics (MD) simulations.[6,11] As the membranes of mitochondria and the ER are mainly composed of phosphatidylcholines, MD studies have so far largely focused on lipid bilayers consisting of unsaturated phospholipids, such as 1,2-dioleoyl-*sn*-glycero-3-phosphocholine (DOPC)[5,6] and 1-palmitoyl-2-oleoyl-*sn*-glycero-3-phosphocholine (POPC),[9,11,19,20] and membrane-mimicking models.[16] A recent study on membrane anchored aromatase considered the more complex composition of the ER membrane.[21] However, to date, no systematic study into the effect of membrane composition on the positioning of CYP has been published.

The ER membrane comprises glycerolipids, such as phosphatidylcholine (PC), phosphatidylethanolamine (PE), phosphatidylinositol (PI), and phosphatidylserine (PS), as well as cholesterol, cardiolipin, and sphingomyelin.[22] Among these lipids, cholesterol is known to significantly alter membrane properties by (i) enhancing the stiffness,[23] (ii) decreasing lateral diffusion,[24,25] (iii) causing "thickening" of the membrane with increasing cholesterol content,[26,27] and (iv) increasing membrane ordering.[28] The presence of cholesterol in the membrane also affects solute partitioning between the membrane and water[29,30] and interactions with proteins.[31] In eukaryotes, the membrane content of cholesterol varies depending on location: the smallest amount is present in the

Received: October 27, 2014
Published: February 5, 2015

DOI: 10.1021/ci500645k
J. Chem. Inf. Model. 2015, 55, 628−635

mitochondrial membrane (3 wt%, 6 mol%), followed by the ER (6 wt%), whereas the largest amount occurs in the plasma membrane (20 wt%).[32] There is also some evidence that the concentration of cholesterol is not homogeneous in membranes and can be locally higher, i.e., in structures called lipid rafts, where cholesterol may also interact with proteins.[31,33,34] The cholesterol gradient from the ER to the cell surface can also regulate sorting of membrane proteins to their correct membrane site.[35] As cholesterol significantly influences membrane properties, it is plausible that it may also affect the structure, orientation, and dynamics of CYP on membranes and in turn the interaction of CYP with its substrates. Recently, Park and co-workers[36] showed that individual CYPs differed in localization in ordered and disordered membrane domains, which had various cholesterol concentrations.

We conducted MD simulations to analyze the structure of CYP3A4 attached to DOPC bilayers with various concentrations of cholesterol (0, 3, 6, 20, and 50 wt%). We chose CYP3A4, as it plays a prominent role in the metabolism of the more than 50% of marketed drugs and is the most abundant CYP in human hepatocytes.[37] CYP3A4 has a deeply buried, large, and malleable active site,[38−40] which can be occupied by more than one ligand.[41−43] It should be noted that cholesterol acts as a CYP3A4 substrate, undergoing 4β-hydroxylation.[44] On the other hand, cholesterol also inhibits several CYP3A4 reactions in a noncompetitive manner.[45] Our MD simulations showed that the presence of cholesterol changes the orientation and rigidifies the membrane-immersed parts of CYP3A4, which could inhibit entry of lipophilic substrates directly from the membrane.

METHODS

Structures. The structure of the catalytic domain of CYP3A4[38] was taken from the Protein Data Bank (PDB ID 1TQN), and the N-terminal anchor, which was missing in the X-ray structure, was added to the structure as an α-helix using methodology described in detail elsewhere.[6] We prepared five lipid bilayers: one consisting of pure DOPC and four composed of DOPC and various (3, 6, 20, and 50 wt%) concentrations of cholesterol. CYP3A4 was inserted into the equilibrated bilayers using the GROMACS tool g_membed.[46] CYP3A4 anchored to the bilayer was then immersed into a rectangular periodic box and solvated by SPC/E[47] explicit water molecules (~30 000). Counter ions were added to maintain a physiological concentration of 0.1 mol/L in the water phase.

MD Procedure. All simulations were carried out with using the Gromacs 4.5.4 program package.[48] We used the Berger lipid force field[49] for the membrane, which was compatible with the GROMOS 53a6[50] force field used for CYP3A4. The lipid bilayer was initially simulated without protein for 200 ns. After the protein was embedded in the membrane, all systems were minimized with the steepest descent method, followed by a short (10 ns long) MD simulation with positional restraints applied on Cα atoms. Afterward, a 200 ns long MD simulation of each system was carried out. Parameters of the MD simulations were set as follows: integration time step, 2 fs with the LINCS algorithm; Berendsen pressure coupling, semi-isotropic Berendsen barostat with pressure 1 bar; isothermal compressibility, 4.5×10^{-5} bar^{-1}; and for temperature coupling, V-rescale thermostat at 310 K with 0.1 ps time constant. The long-range electrostatics was treated with the particle mesh Ewald method, and a pair-list was generated with the group cut-off scheme.

Analysis. As equilibration of systems with CYPs requires at least 50 ns,[6] the first 100 ns of the simulation was set aside for equilibration of CYP3A4, and only data for the last 100 ns were analyzed. For analysis of the membrane properties, we used Gromacs tools.[48] The heme tilt angle was defined as the angle between the heme plane (defined by the heme nitrogens) and the lipid bilayer normal, set as the z axis.[6] Access and egress channels[51] were identified using the MOLE 2.0 tool[52] with the following setup: interior threshold and bottleneck radius, 1.0; probe radius, 8.0; surface cover radius, 3.0; origin radius, 3.0; and starting point located ~3 Å above the heme iron atom (distal side). Water molecules, hydrogens, ions, and membrane atoms were not considered in this analysis. In total, 201 structural snapshots taken every 500 ps (of the last 100 ns) were analyzed. Identified channels were sorted according to the nomenclature introduced by Wade and co-workers,[53] with the exception of channels 2a and 2f, which were united into one channel (henceforth called 2af) because of their high structural similarity.

RESULTS AND DISCUSSION

Addition of Cholesterol Changes the Basic Structural Characteristics of a DOPC Membrane. The presence of cholesterol altered the structure of the DOPC bilayer. DOPC lipid bilayers were generally thicker in the presence of cholesterol, with the headgroup−headgroup distance ($D_{(HH)}$) changing from 4.2 nm in the case of a pure DOPC membrane to 4.6 nm for a membrane containing 20 wt% cholesterol (Table 1). The area per lipid (APL) decreased from 0.59 to 0.42 nm^2. Density profiles also showed that the presence of cholesterol increased the density of the lipid plateau region in terms of the maximal density in the membrane headgroups but did not alter the density in the middle of the membrane

Table 1. Mean Distances of Phosphate (d_P), Cholesterol OH Group (d_{OH}), and Heme Cofactor (d_{heme}) from the Bilayer Center, Area Per Lipid (APL), Average Order Parameters of Lipid Tails ($S_{<CD>}$), Average Fraction of Gauche Bonds (f_g), Heme and Transmembrane (TM) Helix Tilt Angles, and Number of Amino Acid Residues (N) Buried in the Hydrophobic Membrane Interior (below DOPC Carbonyls)

	cholesterol content (wt%)				
	0%	3%	6%	20%	50%
	Membranes without CYP				
d_P (nm)	2.1	2.1	2.1	2.3	2.2
d_{OH} (nm)	–	1.6	1.6	1.8	1.9
APL (nm^2)	0.59	0.58	0.54	0.48	0.42
$S_{<CD>}$	0.182	0.190	0.219	0.259	0.294
f_g	0.157	0.156	0.154	0.150	0.147
	Membranes with CYP				
d_P (nm)	2.0	2.1	2.2	2.3	2.1
d_{OH} (nm)	–	1.5	1.5	1.8	1.8
$S_{<CD>}$	0.172	0.188	0.201	0.246	0.270
f_g	0.156	0.154	0.152	0.148	0.144
d_{heme} (nm)	3.8 ± 0.1	3.7 ± 0.1	3.5 ± 01	3.7 ± 0.1	3.5 ± 0.1
heme tilt angle (deg)	52 ± 8	59 ± 3	60 ± 4	69 ± 5	68 ± 4
TM helix tilt angle (deg)	8 ± 4	10 ± 4	11 ± 4	12 ± 5	9 ± 4
N	54	60	82	79	73

DOI: 10.1021/ci500645k
J. Chem. Inf. Model. 2015, 55, 628−635

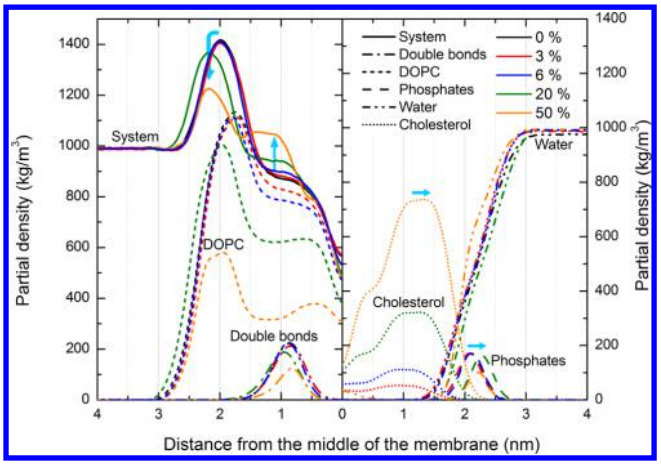

Figure 1. Density profiles of the studied membrane system (without CYP). The membrane was averaged and considered to be symmetric. However, for clarity, the partial densities of groups are shown for just one leaflet.

(Figure 1). As the concentration of cholesterol was increased, the cholesterol OH group shifted further from the membrane center. All these findings are in agreement with previous simulations[25,54,55] and experimental data[55] and confirm that the force field used adequately represented the structural properties of these mixed membranes. Thus, the membrane model was considered valid and used to study the effect of cholesterol content on CYP3A4 anchoring.

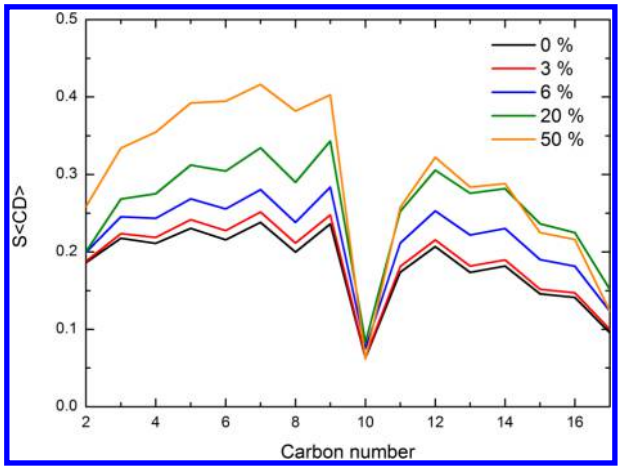

Figure 2. Average order parameter $S_{<CD>}$ for the carbon atoms of DOPC lipid tails calculated from MD simulations with varying cholesterol concentrations.

The presence of cholesterol also induced higher ordering of the DOPC lipid tails (Figure 2). A pure DOPC membrane comprises a diunsaturated lipid with a phase transition temperature of ~255 K[56] and is therefore fluid at ambient temperatures, as documented by the rather low mean order parameter $S_{<CD>}$ of 0.182. Ordering of the lipid membrane was found to increase with increasing cholesterol content, together with a decrease in the fraction of gauche torsion angles of the DOPC lipid chains (Table 1). Higher ordering (above ~0.25) can occur in a liquid-ordered lipid phase, which is generally a cholesterol-rich domain.[25,30,55,57]

Cholesterol Interacts with the N-Terminal Anchor and F/G-Loop of CYP3A4. The simulations showed that CYP3A4 was attached to the membrane by the N-terminal anchor helix, which intersected the membrane, and its catalytic domain was partially immersed in the membrane. The DOPC head groups are pushed aside and DOPC molecules form a funnel-like shape in the membrane occupied by the protein. The N-terminal helix tilt angle, i.e., angle between the helix axis and bilayer normal, was ~10° and was rather insensitive to the cholesterol content (Table 1). This angle is smaller than the transmembrane anchor tilt angle of 17° recently measured by NMR on CYP2B4 anchored to DMPC/DHPC bicelles,[15] which makes sense as the latter lipids have shorter tails and head-to-head distance than DOPC.

The radial distribution function (RDF) of the anchor and cholesterol centers of mass (COMs) showed that cholesterol had some tendency to accumulate in the vicinity of the anchor (Figure 3). Cholesterol also accumulated close to the immersed F/G loop (Figure 4). The number of hydrogen bonds between lipids and CYP3A4 rose with cholesterol content (Table S1) and cholesterol had higher capacity to make hydrogen bonds to membrane buried amino acids. Neither cholesterol nor DOPC molecules penetrated into the protein and stayed in the membrane. Fluctuations of the lipids around CYP were massively reduced (Figure S2 in Supporting Information).

Orientation and Immersion Depth of CYP3A4 on DOPC Membrane Is Affected by the Presence of Cholesterol. The presence of cholesterol in the membrane changed the penetration depth of CYP3A4 in the membrane. Besides the mentioned N-terminal anchor, the F/G loop (bearing F′ and G′ helices) was buried in the lipophilic membrane interior of the pure DOPC membrane (Figure 5). The β1 and β2-sheets, B/C loop, F and G helices, and tip of the I helix interacted with the lipid head groups in same positions as reported earlier.[6] It is worth noting that despite some differences in membrane immersion depths and orientations of individual CYPs, all recent studies have consistently reported insertion of the N-terminal, F′, and G′ helices into the membrane interior,[9,11,16,21] while the B/C loop and F and G helices in CYP3A4[11] have been reported to interact with the membrane. Figure 5 shows that with increasing content of cholesterol, the F and G helices and B/C loop become systematically sunk deeper into the membrane interior. The number of amino acids in contact with the membrane (Tables 1 and S2 in Supporting Information) was the lowest in the pure DOPC membrane and reached a maximum at 6 wt% cholesterol content.

The orientation of the CYP3A4 catalytic domain with respect to the membrane changed with the increasing content of cholesterol in the DOPC membrane (Figure 6), as evaluated from the heme tilt angle (see Methods for definition). The tilt angle systematically increased from 52° in the pure DOPC membrane to 68° in membranes containing 50 wt% cholesterol (Table 1). It should be noted that the experimentally measured tilt angle of CYP3A4 on POPC nanodiscs is $(60 \pm 4)°$.[16] A higher cholesterol content in the DOPC membrane led to increased contact of the CYP3A4 catalytic domain with the membrane, mostly in the vicinity of the F and G helices and β-finger (containing β4 and β5 sheets, and β4/β5 loop). However, the secondary structural elements of the CYP3A4 catalytic domain did not significantly change with increasing cholesterol content (Figures S1 and S3 in Supporting Information).

Cholesterol Presence in the Membrane Alters Active-Site Access Channels Openings. CYP3A4 active-site access

DOI: 10.1021/ci500645k
J. Chem. Inf. Model. 2015, 55, 628−635

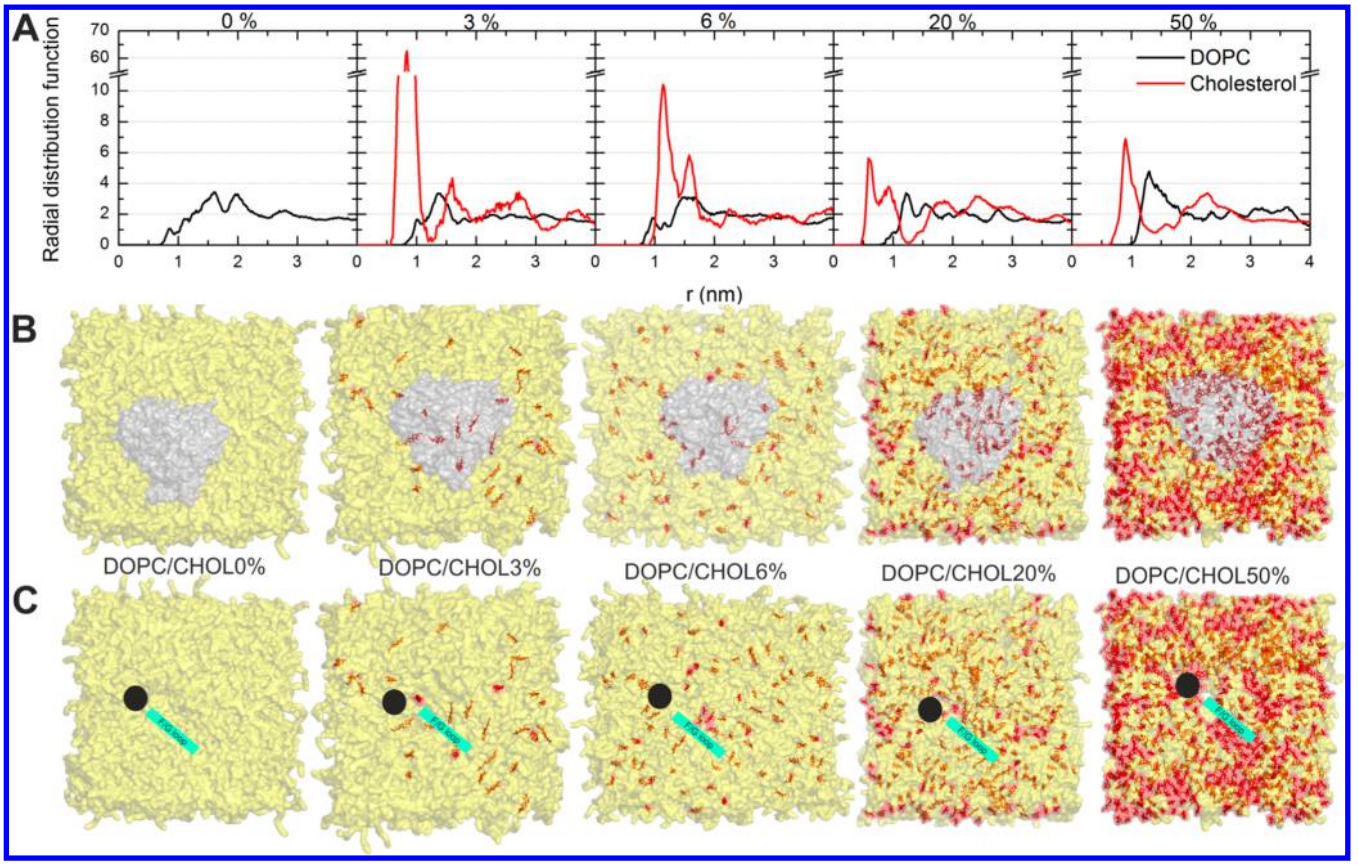

Figure 3. Distribution of cholesterol in membranes. (A) Radial distribution functions of the COMs of DOPC and cholesterol with respect to the transmembrane anchor. (B) Positions of cholesterol molecules (red) in membranes (yellow) with immersed CYP3A4 (gray); frames were taken from 200 ns snapshots. (C) The same view but with CYP3A4 deleted for clarity; positions of the CYP3A4 anchor (black circle) and F/G-loop (green) are shown. Cholesterol showed some tendency to concentrate close to the transmembrane anchor and F/G-loop.

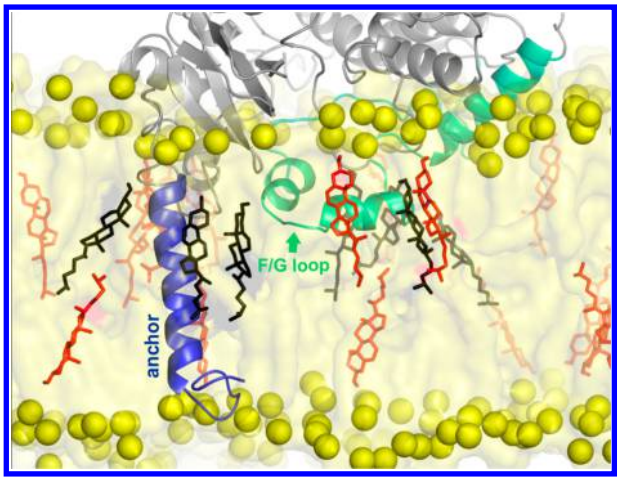

Figure 4. Snapshot taken from MD simulation of CYP3A4 embedded in 6 wt% cholesterol in DOPC membrane showing a typical view of cholesterol molecules interacting with the N-terminal anchor (blue) and F/G loop (green). Membrane phosphates are represented by yellow spheres, cholesterol molecules within 5 Å of CYP3A4 by black sticks and more distal cholesterol molecules by red sticks.

channels connected the active site to both membrane and water phases because their openings were localized inside, on and outside the membrane (Figure 7). The channels 2af, 2b, 2c (around F/G loop), and 4 (through F/G loop) pointed toward the hydrophobic membrane interior. The solvent channel (S; between F, I helices and β-finger) and channels 2e (running through B/C loop) and 3 (between F and G helices) were open to the membrane/water interface. The water channel (W; leading to the proximal side around B, C helices or B/C loop) and channels 1 (among C, H, and L helices) and 5 (between K and K′ helices) opened into the water phase. The positions of these channels are in good agreement with previously published data.[5,6,9] The channels were hydrated and enabled traffic of water molecules in/out CYP3A4 active site (Table S4).

The addition of cholesterol to the DOPC membrane changed the pattern of channel openings. At low cholesterol content (3 and 6 wt%), the water channel was closed and the solvent channel open, but there were no significant changes in the channels pointing to the membrane interior. Channels leading deepest into the membrane, i.e., channels 2af and 2b, closed when CYP was embedded into the cholesterol-rich membrane (with 20 and 50 wt% cholesterol content). The bottlenecks of membrane-exposed channels were narrower in cholesterol rich membranes (Table 2). As well as closure of the channels leading to the membrane, channels leading to the membrane/water interface, such as channels 2e or the solvent channel, opened. Channels leading toward the water phase were highly hydrated (Table S4) and enabled traffic of water molecules out/in CYP3A4 active site. A new channel, labeled 7, whose opening pointed toward the water phase, was identified. Channel 7 passed near the K helix and K/L loop to the proximal side of CYP 3A4 (Figure S2 in Supporting Information). The opening of this channel was caused by subtle movement of the F/G loop and K and L helices.

DOI: 10.1021/ci500645k
J. Chem. Inf. Model. 2015, 55, 628−635

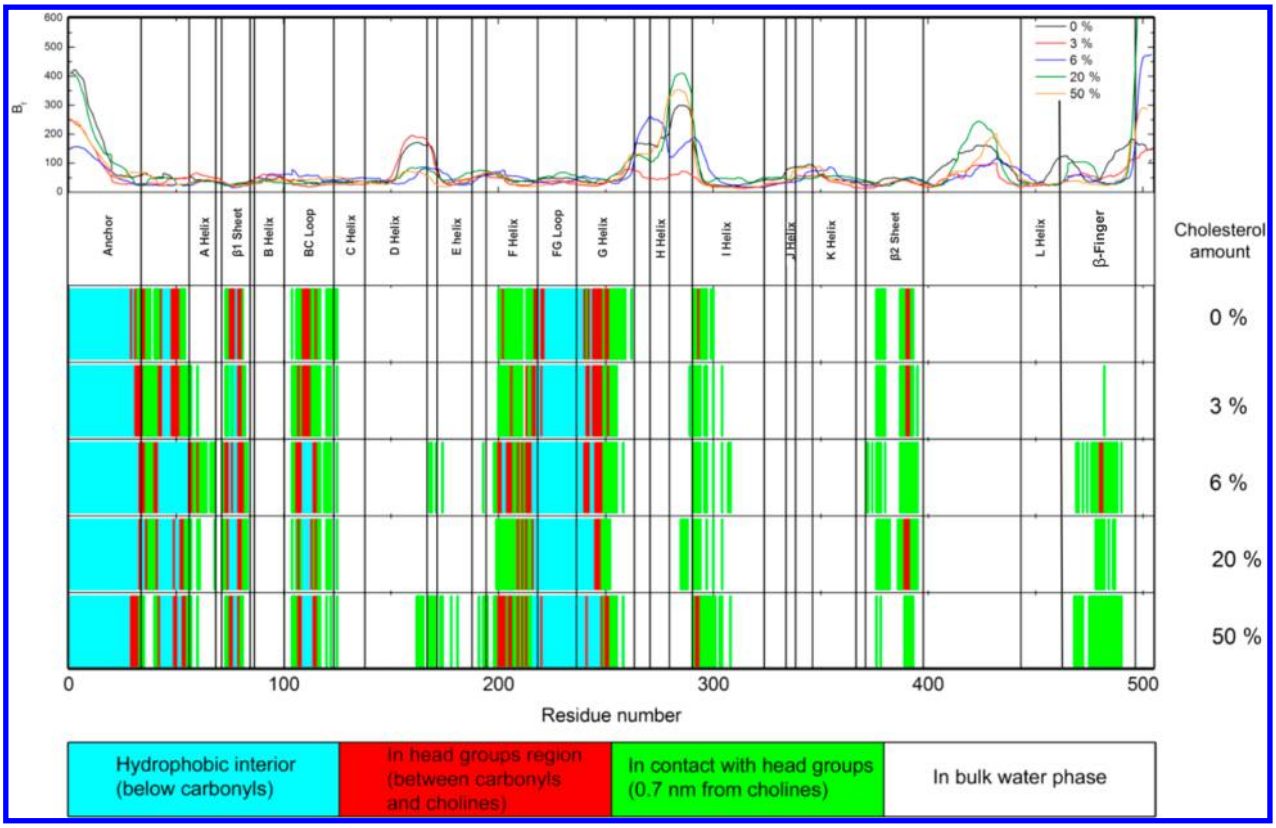

Figure 5. Structural features of CYP3A4 in different membranes. The average B-factors (upper panel) along the protein chain show that the regions in contact with water are the most flexible. The locations of residues differ with respect to the membrane composition (bottom): higher cholesterol leads to more immersed CYP structures, especially in the B/C and F/G loop regions. The colors indicate CYP3A4 parts that are in direct contact with the hydrophobic membrane interior (blue), interact with membrane head groups, i.e., between carbonyl groups and cholines (red), and contact the membrane upper layer (green). The white regions indicate parts in contact with bulk water (cytosol).

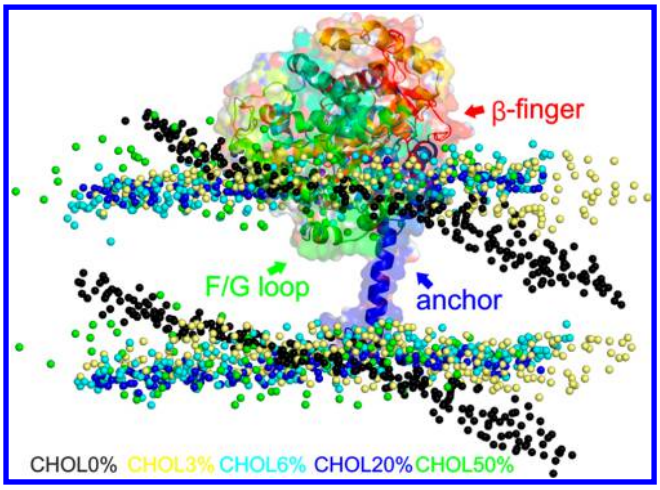

Figure 6. Effect of cholesterol on the orientation of CYP3A4 in the membrane. Structures of CYP3A4 catalytic domain have been superimposed to highlight changes in the CYP34A orientation with respect to the DOPC membrane. The membrane is represented by spheres of phosphorus atoms (for clarity) and colored according to the cholesterol content: 0 wt%, black; 3 wt%, yellow; 6 wt%, cyan; 20 wt%, blue; and 50 wt%, green. CYP3A4 is shown as a cartoon with transparent surfaces.

Generally, conformational changes of channel lining amino acid residues and small variations in arrangement of secondary structural elements, which bear the channel lining amino acids can cause channel opening/closing. The subtle movement of the F/G loop toward the membrane and concurrent opening of the K and L helix region in the CYP structures immersed in membranes containing cholesterol lead to opening of the channel 7. Solvent channel opening and closing was mostly connected with the orientation of R212, which closed solvent channel of CYP3A4 immersed to membranes with 0% and 3% of cholesterol, whereas the channel was open in the membrane containing 20% cholesterol.

CONCLUSION

We studied the effect of increasing the cholesterol content in a DOPC membrane on the behavior of membrane-anchored cytochrome P450 3A4 (CYP3A4). The presence of cholesterol in the lipid membrane significantly changed the membrane thickness, ordering, and diffusion. The position and orientation of CYP3A4 on the membrane were also affected by the cholesterol content. With increasing cholesterol concentration, CYP3A4 was immersed about 0.4 nm deeper into the membrane and was more inclined toward the membrane. In addition, the contact area between the catalytic domain and membrane increased. As a result, about 34% more CYP3A4 amino acids were in contact with the membrane. The presence of cholesterol in the membrane also affected opening of the active-site access channels, but the most pronounced changes occurred for high (20 and 50 wt%) cholesterol concentrations. One can hypothesize that the above-discussed changes might also contribute to the noncompetitive inhibition of CYP3A4 by cholesterol observed by Shinkyo and Guengerich.[45] Our results show that cholesterol content significantly influences the

DOI: 10.1021/ci500645k
J. Chem. Inf. Model. 2015, 55, 628−635

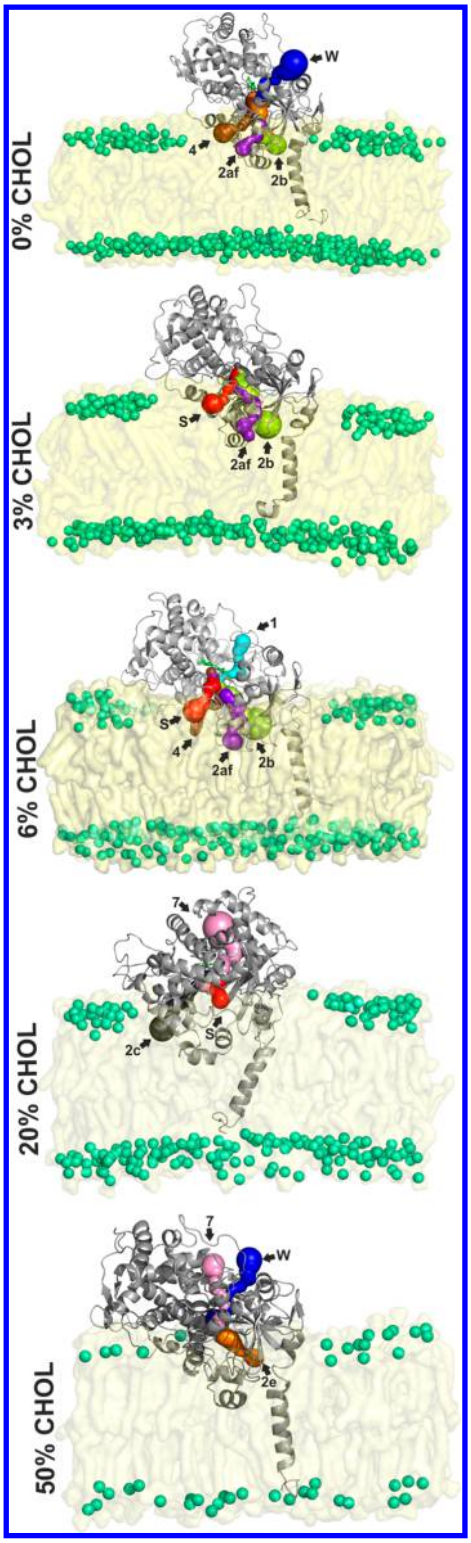

Figure 7. Channel openings (highlighted by arrows) of CYP3A4 active-site access channels (open with bottleneck radius of 1 Å and higher in 15% of frames) are shown in DOPC membranes with increasing cholesterol content. Access channels are labeled according to the nomenclature introduced by Wade and co-workers,[53] and colored as follows: 1, cyan; 4, brown; 7, pink; W, blue; S, red; 2af, magenta; 2b, bright green; 2c, gray; 2e, orange. Membrane lipids are represented as transparent surfaces and phosphates in green spheres; CYP3A4 is shown as a cartoon.

Table 2. Normalized Frequency of CYP Channel Opening (nfreq) and Average Radius (Rmax) of Bottlenecks[a]

		chol 0%		chol 3%		chol 6%		chol 20%		chol 50%	
	#	nfreq	Rmax	nfreq	Rmax	nfreq	Rmax	nfreq	Rmax	nfreq	Rmax
membrane	2af	47	1.46	30	1.45	29	1.39	2	1.19	4	1.24
	2b	76	1.73	95	1.64	88	1.53	1	1.09	10	1.41
	4	18	1.29	8	1.26	17	1.31	1	1.16	11	1.31
interface	2c	5	1.42	1	1.13			21	1.43	4	1.26
	2e	33	1.61	1	1.01	2	1.13	78	1.77	62	1.59
	S			27	1.28	45	1.47	75	1.89	5	1.17
	3	5	1.22			2	1.01	2	1.05	1	1.2
	5							9	1.39	5	1.23
water	1	10	1.25	2	1.17	20	1.36	10	1.47	10	1.24
	W	56	1.38	5	1.27	3	1.07	1	1.01	21	1.36
	7					11	1.62	34	1.57	78	1.55
	r	0.74		0.89		0.62		0.92		0.90	

[a]Rmax values are colored according to their bottleneck radius, from dark green for the most open to red for the most closed channels. According to the Rmax and nfreq values, the most frequently occurring channels were also the most open, whereas rarely observed channels tended to have rather narrow bottlenecks. The last line shows the correlation coefficients between nfreq and Rmax.

structural features of a membrane-anchored enzyme, which in turn may affect the substrate preferences and catalytic efficiency of the respective membranes or membrane domains. The described changes may influence biotransformation processes in different membrane parts and various cellular compartments, which differ in membrane composition and cholesterol content.

■ ASSOCIATED CONTENT

Supporting Information

Root-mean-square fluctuations of the systems with different cholesterol content (Figure S1); detailed view of newly observed channel 7 (Figure S2); number of hydrogen bonds between lipids, protein, and water (Table S1); numbers of protein residues located in various parts of the membrane and potentially interacting with the membrane (Table S2); numbers of solvent and ions in the simulated system (Table S3); number of water molecules in various channels (Table S4); evolution of secondary structure elements (Figure S3); overview of all channels found in the CYPs in membranes with different cholesterol content (Figure S4). This material is available free of charge via the Internet at http://pubs.acs.org.

■ AUTHOR INFORMATION

Corresponding Authors

*K.B.: phone +420 585634769, fax +420 585634761, E-mail karel.berka@upol.cz.

*M.O.: phone +420 585634756, fax +420 585634761, E-mail michal.otyepka@upol.cz.

Notes

The authors declare no competing financial interest.

■ ACKNOWLEDGMENTS

This research was supported by the Operational Program Research and Development for Innovations—European Social Fund (CZ.1.07/2.4.00/31.0130 ChemPharmNet) from the Ministry of Education Youth and Sports, Czech Republic. We acknowledge support from the Czech Grant Agency through the projects P303/12/P019 to K.B. and P208/12/G016 to M.O. We also acknowledge support from a student project of Palacký University Olomouc (IGA_PrF_2014023) to M.P. and V.N. The authors gratefully acknowledge support through the

DOI: 10.1021/ci500645k
J. Chem. Inf. Model. 2015, 55, 628−635

project LO1305 of the Ministry of Education, Youth and Sports of the Czech Republic.

■ ABBREVIATIONS

CYP, cytochrome P450; ER, endoplasmic reticulum; DOPC, 1,2-dioleoyl-*sn*-glycero-3-phosphocholine; POPC, 1-palmitoyl-2-oleoyl-*sn*-glycero-3-phosphocholine; MD, molecular dynamics; PC, phosphatidylcholine; PE, phosphatidylethanolamine; PI, phosphatidylinositol; PS, phosphatidylserine; APL, area per lipid; TM, transmembrane; DMPC, 1,2-dimyristoyl-*sn*-glycero-3-phosphocholine; DHCP, 1,2-diheptanoyl-*sn*-glycero-3-phosphocholine; CHOL, cholesterol; RDF, radial distribution function; COM, center of mass

■ REFERENCES

(1) Guengerich, F. P. Common and Uncommon Cytochrome P450 Reactions Related to Metabolism and Chemical Toxicity. *Chem. Res. Toxicol.* **2001**, *14*, 611−650.
(2) Ortiz de Montellano, P. R., Ed. *Cytochrome P450: Structure, Mechanism, and Biochemistry*, 3rd ed.; Kluwer Academic/Plenum Publishers: New York, 2005; Vol. *21*, p 690.
(3) Black, S. D. Membrane Topology of the Mammalian P450 Cytochromes. *FASEB J.* **1992**, *6*, 680−685.
(4) Williams, P. A.; Cosme, J.; Sridhar, V.; Johnson, E. F.; McRee, D. E. Microsomal Cytochrome P450 2C5: Comparison to Microbial P450s and Unique Features. *J. Inorg. Biochem.* **2000**, *81*, 183−190.
(5) Berka, K.; Hendrychová, T.; Anzenbacher, P.; Otyepka, M. Membrane Position of Ibuprofen Agrees with Suggested Access Path Entrance to Cytochrome P450 2C9 Active Site. *J. Phys. Chem. A* **2011**, *115*, 11248−11255.
(6) Berka, K.; Paloncýová, M.; Anzenbacher, P.; Otyepka, M. Behavior of Human Cytochromes P450 on Lipid Membranes. *J. Phys. Chem. B* **2013**, *117*, 11556−11564.
(7) Endo, S.; Escher, B. I.; Goss, K.-U. Capacities of Membrane Lipids to Accumulate Neutral Organic Chemicals. *Environ. Sci. Technol.* **2011**, *45*, 5912−5921.
(8) Paloncýová, M.; Devane, R.; Murch, B.; Berka, K.; Otyepka, M. Amphiphilic Drug-Like Molecules Accumulate in a Membrane below the Head Group Region. *J. Phys. Chem. B* **2014**, *118*, 1030−1039.
(9) Cojocaru, V.; Balali-Mood, K.; Sansom, M. S. P.; Wade, R. C. Structure and Dynamics of the Membrane-Bound Cytochrome P450 2C9. *PLoS Comput. Biol.* **2011**, *7*, No. e1002152.
(10) Kingsley, L. J.; Lill, M. a Ensemble Generation and the Influence of Protein Flexibility on Geometric Tunnel Prediction in Cytochrome P450 Enzymes. *PLoS One* **2014**, *9*, No. e99408.
(11) Denisov, I. G.; Shih, a Y.; Sligar, S. G. Structural Differences between Soluble and Membrane Bound Cytochrome P450s. *J. Inorg. Biochem.* **2012**, *108*, 150−158.
(12) Sündermann, A.; Oostenbrink, C. Molecular Dynamics Simulations Give Insight into the Conformational Change, Complex Formation, and Electron Transfer Pathway for Cytochrome P450 Reductase. *Protein Sci.* **2013**, *22*, 1183−1195.
(13) Yamamoto, K.; Dürr, U. H. N.; Xu, J.; Im, S.-C.; Waskell, L.; Ramamoorthy, A. Dynamic Interaction between Membrane-Bound Full-Length Cytochrome P450 and Cytochrome b5 Observed by Solid-State NMR Spectroscopy. *Sci. Rep.* **2013**, *3*, No. 2538.
(14) Dürr, U. H. N.; Waskell, L.; Ramamoorthy, A. The Cytochromes P450 and b5 and their Reductases—Promising Targets for Structural Studies by Advanced Solid-State NMR Spectroscopy. *Biochim. Biophys. Acta* **2007**, *1768*, 3235−3259.
(15) Yamamoto, K.; Gildenberg, M.; Ahuja, S.; Im, S.-C.; Pearcy, P.; Waskell, L.; Ramamoorthy, A. Probing the Transmembrane Structure and Topology of Microsomal Cytochrome-P450 by Solid-State NMR on Temperature-Resistant Bicelles. *Sci. Rep.* **2013**, *3*, No. 2556.
(16) Baylon, J. L.; Lenov, I. L.; Sligar, S. G.; Tajkhorshid, E. Characterizing the Membrane-Bound State of Cytochrome P450 3A4: Structure, Depth of Insertion and Orientation. *J. Am. Chem. Soc.* **2013**, *135*, 8542−8551.
(17) Williams, P. A.; Cosme, J.; Sridhar, V.; Johnson, E. F.; McRee, D. E. Mammalian Microsomal Cytochrome P450 Monooxygenase: Structural Adaptations for Membrane Binding and Functional Diversity. *Mol. Cell* **2000**, *5*, 121−131.
(18) Monk, B. C.; Tomasiak, T. M.; Keniya, M. V.; Huschmann, F. U.; Tyndall, J. D. A. Architecture of a Single Membrane Spanning Cytochrome P450 Suggests Constraints that Orient the Catalytic Domain Relative to a Bilayer. *Proc. Natl. Acad. Sci. U.S.A.* **2014**, *111*, 3865−3870.
(19) Jiang, W.; Ghosh, D. Motion and Flexibility in Human Cytochrome P450 Aromatase. *PLoS One* **2012**, *7*, No. e32565.
(20) Sgrignani, J.; Magistrato, A. Influence of the Membrane Lipophilic Environment on the Structure and on the Substrate Access/Egress Routes of the Human Aromatase Enzyme. A Computational Study. *J. Chem. Inf. Model.* **2012**, *52*, 1595−1606.
(21) Park, J.; Czapla, L.; Amaro, R. Molecular Simulations of Aromatase Reveal New Insights into the Mechanism of Ligand Binding. *J. Chem. Inf. Model.* **2013**, *53*, 2047−2056.
(22) Van Meer, G.; de Kroon, A. I. P. M. Lipid Map of the Mammalian Cell. *J. Cell Sci.* **2011**, *124*, 5−8.
(23) Needham, D.; McIntosh, T.; Evans, E. Thermomechanical and Transition Properties of Dimyristoylphosphatidylcholine/Cholesterol Bilayers. *Biochemistry* **1988**, 4668−4673.
(24) Evans, E.; Needham, D. Physical Properties of Surfactant Bilayer Membranes: Thermal Transitions, Elasticity, Rigidity, Cohesion and Colloidal Interactions. *J. Phys. Chem.* **1987**, *2*, 4219−4228.
(25) Ohvo-Rekilä, H.; Ramstedt, B.; Leppimäki, P.; Slotte, J. P. Cholesterol Interactions with Phospholipids in Membranes. *Prog. Lipid Res.* **2002**, *41*, 66−97.
(26) Raffy, S.; Teissié, J. Control of Lipid Membrane Stability by Cholesterol Content. *Biophys. J.* **1999**, *76*, 2072−2080.
(27) Drolle, E.; Kučerka, N.; Hoopes, M. I.; Choi, Y.; Katsaras, J.; Karttunen, M.; Leonenko, Z. Effect of Melatonin and Cholesterol on the Structure of DOPC and DPPC Membranes. *Biochim. Biophys. Acta* **2013**, *1828*, 2247−2254.
(28) Hung, W.-C.; Lee, M.-T.; Chen, F.-Y.; Huang, H. W. The Condensing Effect of Cholesterol in Lipid Bilayers. *Biophys. J.* **2007**, *92*, 3960−3967.
(29) Trandum, C.; Westh, P.; Jorgensen, K.; Mouritsen, O. G. A Thermodynamic Study of the Effects of Cholesterol on the Interaction Between Liposomes and Ethanol. *Biophys. J.* **2000**, *78*, 2486−2492.
(30) Wennberg, C. L.; Spoel, D. Van Der; Hub, J. S. Large Influence of Cholesterol on Solute Partitioning into Lipid Membranes. *J. Am. Chem. Soc.* **2012**, *134*, 5351−5361.
(31) Pike, L. J. The Challenge of Lipid Rafts. *J. Lipid Res.* **2009**, *50* (Suppl), S323−328.
(32) Sackman, E. Biological Membranes Architecture and Function. In *Structure and Dynamics of Membranes From Cells to Vesicles*; Lipowsky, R., Sackmann, E., Eds.; Elsevier: Amsterdam, 1995; pp 1−63.
(33) Epand, R. M. Cholesterol and the Interaction of Proteins with Membrane Domains. *Prog. Lipid Res.* **2006**, *45*, 279−294.
(34) Fantini, J. Interaction of Proteins with Lipid Rafts through Glycolipid-Binding Domains: Biochemical Background and Potential Therapeutic Applications. *Curr. Med. Chem.* **2007**, *14*, 2911−2917.
(35) Coskun, Ü.; Simons, K. Cell Membranes: the Lipid Perspective. *Structure* **2011**, *19*, 1543−1548.
(36) Park, J. W.; Reed, J. R.; Brignac-Huber, L. M.; Backes, W. L. Cytochrome P450 System Proteins Reside in Different Regions of the Endoplasmic Reticulum. *Biochem. J.* **2014**, *464*, 241−249.
(37) Anzenbacher, P.; Anzenbacherová, E. Cytochromes P450 and Metabolism of Xenobiotics. *Cell. Mol. Life Sci.* **2001**, *58*, 737−747.
(38) Yano, J. K.; Wester, M. R.; Schoch, G. A.; Griffin, K. J.; Stout, C. D.; Johnson, E. F. The Structure of Human Microsomal Cytochrome P450 3A4 Determined by X-ray Crystallography to 2.05-A Resolution. *J. Biol. Chem.* **2004**, *279*, 38091−38094.

DOI: 10.1021/ci500645k
J. Chem. Inf. Model. 2015, 55, 628−635

(39) Otyepka, M.; Skopalík, J.; Anzenbacherová, E.; Anzenbacher, P. What Common Structural Features and Variations of Mammalian P450s Are Known to Date? *Biochim. Biophys. Acta* **2007**, *1770*, 376−389.
(40) Hendrychová, T.; Anzenbacherová, E.; Hudeček, J.; Skopalík, J.; Lange, R.; Hildebrandt, P.; Otyepka, M.; Anzenbacher, P. Flexibility of Human Cytochrome P450 Enzymes: Molecular Dynamics and Spectroscopy Reveal Important Function-Related Variations. *Biochim. Biophys. Acta* **2011**, *1814*, 58−68.
(41) Bren, U.; Oostenbrink, C. Cytochrome P450 3A4 Inhibition by Ketoconazole: Tackling the Problem of Ligand Cooperativity Using Molecular Dynamics Simulations and Free-Energy Calculations. *J. Chem. Inf. Model.* **2012**, *52*, 1573−1582.
(42) Bren, U.; Fuchs, J. E.; Oostenbrink, C. Cooperative Binding of Aflatoxin B 1 by Cytochrome P450 3A4: A Computational Study. *Chem. Res. Toxicol.* **2014**, *27*, 2136−2147.
(43) Davydov, D. R.; Halpert, J. R. Allosteric P450 Mechanisms: Multiple Binding Sites, Multiple Conformers, or Both? *Exp. Opin. Drug Metab. Toxicol.* **2008**, *4*, 1523−1535.
(44) Bodin, K.; Bretillon, L.; Aden, Y.; Bertilsson, L.; Broomé, U.; Einarsson, C.; Diczfalusy, U. Antiepileptic Drugs Increase Plasma Levels of 4beta-Hydroxycholesterol in Humans: Evidence for Involvement of Cytochrome P450 3A4. *J. Biol. Chem.* **2001**, *276*, 38685−38689.
(45) Shinkyo, R.; Guengerich, F. P. Inhibition of Human Cytochrome P450 3A4 by Cholesterol. *J. Biol. Chem.* **2011**, *286*, 18426−18433.
(46) Wolf, M. G.; Hoefling, M.; Aponte-Santamaría, C.; Grubmüller, H.; Groenhof, G. g _ membed: Efficient Insertion of a Membrane Protein into an Equilibrated Lipid Bilayer with Minimal Perturbation. *J. Comput. Chem.* **2010**, *31*, 2160−2174.
(47) Berendsen, H. The Missing Term in Effective Pair Potentials. *J. Phys. Chem.* **1987**, *91*, 6269−6271.
(48) Hess, B.; Kutzner, C.; van der Spoel, D.; Lindahl, E. GROMACS 4: Algorithms for Highly Efficient, Load-Balanced, and Scalable Molecular Simulation. *J. Chem. Theory Comput.* **2008**, *4*, 435−447.
(49) Berger, O.; Edholm, O.; Jahnig, F. Molecular Dynamics Simulations of a Fluid Bilayer of Dipalmitoylphosphatidylcholine at Full Hydration, Constant Pressure and Constant Temperature. *Biophys. J.* **1997**, *72*, 2002−2013.
(50) Oostenbrink, C.; Villa, A.; Mark, A. E.; van Gunsteren, W. F. A Biomolecular Force Field Based on the Free Enthalpy of Hydration and Solvation: the GROMOS Force-Field Parameter Sets 53A5 and 53A6. *J. Comput. Chem.* **2004**, *25*, 1656−1676.
(51) Pravda, L.; Berka, K.; Svobodová Vařeková, R.; Sehnal, D.; Banáš, P.; Laskowski, R. A.; Koča, J.; Otyepka, M. Anatomy of enzyme channels. *BMC Bioinformatics* **2014**, *15*, 379.
(52) Sehnal, D.; Svobodová Vařeková, R.; Berka, K.; Pravda, L.; Navrátilová, V.; Banáš, P.; Ionescu, C.-M.; Otyepka, M.; Koča, J. MOLE 2.0: Advanced Approach for Analysis of Biomacromolecular Channels. *J. Cheminform.* **2013**, *5*, 39.
(53) Cojocaru, V.; Winn, P. J.; Wade, R. C. The Ins and Outs of Cytochrome P450s. *Biochim. Biophys. Acta* **2007**, *1770*, 390−401.
(54) Hofsäss, C.; Lindahl, E.; Edholm, O. Molecular Dynamics Simulations of Phospholipid Bilayers with Cholesterol. *Biophys. J.* **2003**, *84*, 2192−2206.
(55) Róg, T.; Pasenkiewicz-Gierula, M.; Vattulainen, I.; Karttunen, M. Ordering Effects of Cholesterol and its Analogues. *Biochim. Biophys. Acta* **2009**, *1788*, 97−121.
(56) Koynova, R.; Caffrey, M. Phases and Phase Transitions of the Phosphatidylcholines. *Biochim. Biophys. Acta* **1998**, *1376*, 91−145.
(57) Rawicz, W.; Smith, B. A.; McIntosh, T. J.; Simon, S. A.; Evans, E. Elasticity, Strength, and Water Permeability of Bilayers that Contain Raft Microdomain-Forming Lipids. *Biophys. J.* **2008**, *94*, 4725−4736.

DOI: 10.1021/ci500645k
J. Chem. Inf. Model. 2015, 55, 628−635